A density matrix functional with occupation number driven treatment of dynamical and nondynamical correlation

Rohr, D.; Pernal, K.D.; Gritsenko, O.V.; Baerends, E.J.

published in
Journal of Chemical Physics
2008

DOI (link to publisher)
10.1063/1.2998201

document version
Publisher's PDF, also known as Version of record

A density matrix functional with occupation number driven treatment of dynamical and nondynamical correlation

Daniel R. Rohr,[1] Katarzyna Pernal,[1,2] Oleg V. Gritsenko,[1] and Evert Jan Baerends[1,a)]
[1]*Afdeling Theoretische Chemie, Vrije Universiteit, De Boelelaan 1083, 1081 HV Amsterdam, The Netherlands*
[2]*Institute of Physics, Technical University of Lodz, ul. Wolczanska 219, 93-005 Lodz, Poland*

(Received 6 August 2008; accepted 19 September 2008; published online 23 October 2008)

A recently proposed series of corrections to the earliest *JK*-only functionals has considerably improved the prospects of density matrix functional theory (DMFT). Still, the most advanced of these functionals (correction *C*3) requires a preselection of the terms in the pair density $\Gamma(\mathbf{r}_1,\mathbf{r}_2)$ involving the bonding and antibonding natural orbitals (NOs) belonging to an electron pair bond. Ideally, a DMFT functional should only depend on the NOs and their occupation numbers, and we propose a functional with an occupation number driven weighing of terms in the pair density. These are formulated as "damping" for certain ranges of occupation numbers of the two-electron cumulant that arises in the expansion of the two-particle density matrix of the paradigmatic two-electron system. This automatic version of *C*3, which we denote *AC*3, provides the correct dissociation limit for electron pair bonds and it excellently reproduces the potential energy curves of the multireference configuration interaction (MRCI) method for the dissociation of the electron pair bond in the series of the ten-electron hydrides CH_4, NH_3, H_2O, and HF. *AC*3 reproduces closely the experimental equilibrium distances and at R_e it yields correlation energies of the ten-electron systems with an average error in the absolute values of only 3.3% compared to the MRCI values. We stress the importance of treatment of strong correlation cases (NO occupation numbers differing significantly from 2.0 and 0.0) by appropriate terms in the cumulant. © *2008 American Institute of Physics*. [DOI: 10.1063/1.2998201]

I. INTRODUCTION

In density matrix functional theory (DMFT),[1–15] the total electronic energy is considered to be a functional $E[\gamma]$ of the one-particle density matrix (one-matrix) $\gamma(\mathbf{r}_1,\mathbf{r}_1')$,

$$E[\gamma]=E_{oe}[\gamma]+E_{ee}[\gamma], \tag{1.1}$$

$$\gamma(\mathbf{r}_1,\mathbf{r}_1')=\sum_i n_i\chi_i(\mathbf{r}_1')^*\chi_i(\mathbf{r}_1). \tag{1.2}$$

In Eq. (1.2) $\{\chi_i\}$ are the natural orbitals (NOs) with the occupations n_i (we consider only closed shell systems here and the occupation numbers are in the range [0,2]) and $E[\gamma]$ is the sum of the one-electron $E_{oe}[\gamma]$,

$$E_{oe}[\gamma]=-\frac{1}{2}\int [\nabla_{\mathbf{r}_1'}^2\gamma(\mathbf{r}_1,\mathbf{r}_1')]|_{\mathbf{r}_1'=\mathbf{r}_1}d\mathbf{r}_1 + \int v_{\mathrm{ext}}(\mathbf{r}_1)\rho(\mathbf{r}_1)d\mathbf{r}_1, \tag{1.3}$$

and electron-electron interaction $E_{ee}[\gamma]$,

$$E_{ee}[\gamma]=\frac{1}{2}\int\frac{\Gamma([\gamma];\mathbf{r}_1,\mathbf{r}_2)}{|\mathbf{r}_1-\mathbf{r}_2|}d\mathbf{r}_1d\mathbf{r}_2, \tag{1.4}$$

energies (we use atomic units). In Eq. (1.3) $\rho(\mathbf{r}_1)$ is the electron density (diagonal of the one-matrix) and $v_{\mathrm{ext}}(\mathbf{r}_1)$ is the external potential. The exact pair-density functional $\Gamma[\gamma]$ is not known. We use the usual partitioning in Coulomb, exchange, and a rest term ("correlation"),

$$\Gamma([\gamma];\mathbf{r}_1,\mathbf{r}_2)=\rho(\mathbf{r}_1)\rho(\mathbf{r}_2)-\tfrac{1}{2}|\gamma(\mathbf{r}_1,\mathbf{r}_2)|^2+C([\gamma];\mathbf{r}_1,\mathbf{r}_2). \tag{1.5}$$

When in the exchange term the exact one-matrix γ is used, as we will do, instead of the Hartree–Fock density matrix γ^{HF}; the correlation part of the two-electron energy $(1/2)\int C(\mathbf{r}_1,\mathbf{r}_2)d\mathbf{r}_1d\mathbf{r}_2/r_{12}$ is differently defined than in the usual definition of correlation as the energy difference with respect to the Hartree–Fock energy. The partitioning of the energy according to Eq. (1.5) has often been used,[11,16–18] although it has the disadvantage that the sum rule for the exchange hole that it integrates to −1 now no longer holds. (This can be remedied by working with the best idempotent approximant to γ, see Kutzelnigg[19]). It is natural to use Eq. (1.5) when the Hartree–Fock model is not taken as a starting point, but the one-matrix is targeted directly, as in this paper. The correlation term $C[\gamma](\mathbf{r}_1,\mathbf{r}_2)$ is in fact the two-particle cumulant in the well-known cumulant expansion of the two-particle density matrix (two-matrix), and although we will not make any essential use of the cumulant expansion as such (i.e., to higher orders), we will conveniently denote it as the two-electron cumulant henceforth. The two-electron cumulant can be written as

a)Electronic mail: baerends@chem.vu.nl.

$$C([\gamma];\mathbf{r}_1,\mathbf{r}_2)=\sum_{i,j,k,l} c_{ijkl}\chi_i^*(\mathbf{r}_1)\chi_j^*(\mathbf{r}_2)\chi_k(\mathbf{r}_1)\chi_l(\mathbf{r}_2), \quad (1.6a)$$

and the first successful approximations to $C[\gamma]$ have been the so-called *JK*-only functionals,[6,8,9,11,13,20,21] where in the basis of NOs $\{\chi_i\}$ the matrix elements c_{ijkl} are approximated by the "exchangelike" terms

$$c_{ijkl}\approx c_{ij}(n_i,n_j)\delta_{jk}\delta_{il}, \quad (1.6b)$$

leading to *K* integrals in the energy expression. Specifically, the *J* integrals are required for the Hartree functional emerging from the first term of Eq. (1.5), while with the approximation (1.6b) only *K* integrals are used for the exchange and correlation (xc) functionals emerging from the last two terms. Reference 8 discusses in detail why the correlation effects (both dynamical and nondynamical) can be described with good accuracy with just *K* integrals, and has demonstrated that the Fermi and Coulomb holes can be modeled accurately with an expression of type (1.6b).

For two-electron systems the $\Gamma[\gamma]$ is known from the work by Löwdin and Shull,[1] i.e., the two-matrix can be written in terms of NOs and NO occupation numbers. After approximating the diagonal terms of this expression, as was indicated in Refs. 8, 11, and 20, the resultant two-electron form $c_{ij}^{(2)}$ of the coefficients in Eq. (1.6b),

$$c_{ij}^{(2)}(n_i,n_j)=f_{ij}\sqrt{n_in_j}+\tfrac{1}{2}n_in_j;$$
$$f_{ij}=\begin{cases}+1, & i,j(\neq i)>N/2\\ -1, & \text{otherwise}\end{cases} \quad (1.7)$$

can serve as a paradigm for DMFT developments. We order the NOs according to descending occupation number, and *N* is the number of electrons. The first $N/2$ NOs typically have high occupations (most are close to 2.0); the remaining ones have low occupations (most are close to 0.0). The $(1/2)n_in_j$ term simply cancels the exchange term in Eq. (1.5), so this expression for the cumulant represents just the $f_{ij}\sqrt{n_in_j}K_{ij}$ exchange-correlation terms in the total energy of the two-electron system. The two-electron cumulant *C* obtained by applying the $c_{ij}^{(2)}$ coefficients of Eq. (1.7) in the *C* of Eq. (1.6) provides a total energy that is not exact for the two-electron systems, but that reproduces very well the electron correlation in prototype two-electron systems such as the He isoelectronic series (dynamical correlation) and the (dissociating) H_2 molecule (nondynamical correlation).[8,11,20] The sign choice that we make here with the f_{ij}, although correct for these important cases for chemistry, is not universally correct for all two-electron systems.[22] [The $c_{ij}^{(2)}$ coefficients are strictly speaking not just functions of the occupation numbers but also of the ordinal numbers of the orbitals *i* and *j* (whether $>$ or $\leq N/2$), in the ordering of the orbitals according to decreasing occupation number; this dependence, which is indeed directly determined by the occupation numbers, is not separately indicated.]

Molecular dissociation, which is an essentially nonlocal phenomenon, presents a challenging problem for the standard local and semilocal functionals of density functional theory (DFT) (Refs. 23 and 24) (see Sec. III for illustration of this problem). The representation of *C* in terms of the delocalized NOs $\{\chi_i\}$ offers in principle an adequate description of such nonlocal phenomena. The first NO functional was derived by Müller[6] from the requirement of minimal violation of the Pauli principle, and by Buijse and Baerends[8,11] from an analysis of Fermi and Coulomb correlation holes, both in the case of dynamical and nondynamical correlation,

$$c_{ij}^{\sqrt{n}}(n_i,n_j)=-\sqrt{n_in_j}+\tfrac{1}{2}n_in_j. \quad (1.8)$$

The term $(1/2)n_in_j$ annihilates the exchange term in Eq. (1.5), so that the $-\sqrt{n_in_j}$ term has to take care of all xc effects. The functional of Eq. (1.8) has variously been called the Müller functional,[25] the Buijse–Baerends (BB) functional,[24,26] and the corrected Hartree functional.[10] We will denote it as the $\sqrt{n}$ functional. It is important for chemistry that this functional, in spite of requiring only *J* and *K* integrals according to Eq. (1.6), in a Hartree–Fock-like energy expression, has been designed to describe properly the prototype correlation (nondynamical as well as dynamical) in systems such as the He-isoelectron series and the (dissociating) H_2 molecule, at least when the NOs and NO occupations are used nonself-consistently.[8,11,20] It is less accurate when NOs and occupations are self-consistently optimized.[27,28] This is presumably caused by the fact that the $\sqrt{n}$ functional deviates too much from the rather accurate two-electron form [Eq. (1.7)].

Various corrections to the $\sqrt{n}$ functional of Eq. (1.8) have been proposed.[9,20,21] Goedecker and Umrigar (GU) (Ref. 9) proposed to omit the diagonal terms ($i=j$ terms) in both the Coulomb and the xc term, which leads to improved total energies of atoms and molecules at R_e but to deterioration at large bond distances.[20,28,29] Gritsenko *et al.*[20] introduced a series of three repulsive corrections *C*1, *C*2, and *C*3 (see below) to the $\sqrt{n}$ functional of Eq. (1.8). The first, *C*1, is just restoring the +1 factors in front of $\sqrt{n_in_j}$ for the off-diagonal virtual-virtual terms ($i,j>N/2$), i.e., it goes back to the two-electron form $c_{ij}^{(2)}$. The correction *C*3 introduces explicitly a special treatment of strong (nondynamical) correlation. Piris and co-worker[21,30] proposed the Piris NO functional (denoted PNOF0), based on a detailed consideration of properties of the cumulant *C*. The PNOF0 functional effectively applies the *C*1 correction in combination with the diagonal GU correction. Piris[30] also introduced an extended form, denoted as PNOF, which prevents pinning of high occupation numbers ($n_i\approx 2$) at 2.0. Lathiotakis and Marques[31] showed, in benchmark calculations of the E_c values for the *G*2 set of molecules with the BBC1–BBC3, PNOF0, PNOF, and ML (see below) functionals, that the simple PNOF0 form performs better than PNOF. We therefore compare our AC3 functional in this paper to the PNOF0 functional. We further compare it to the ML functional, proposed by Marques and Lathiotakis in Ref. 32. In this functional the $\sqrt{n_in_j}$ factor in the $\sqrt{n}$ functional is replaced with a Padé approximant in $x=n_in_j$, the coefficients in the approximant being empirically determined by a fit to reproduce the correlation energies E_c of prototype molecules at the equilibrium geometry. The Padé approximant form implies that only integer powers of the NO occupations are employed in both the numerator and the denomi-

nator of the ML cumulant. The ML functional outperformed all other DMFT functionals for the correlation energy at R_e with the $G2$ benchmark set of molecules in a $6-31G^*$ basis set.[32]

The currently available assessments of these functionals have, with the exception of BBC1–BBC3, been carried out in a rather small basis and only at the equilibrium geometry. In Ref. 20 the full potential energy curves of a few prototype molecules were calculated with the BBC1–BBC3 functionals in a larger basis. The most advanced functional, with the corrections labeled $C3$, reproduces remarkably well the potential energy curves of prototype single-bonded molecules. However, the price for this performance is the dependence of c_{ij}^{C3} not only on $\{n_i\}$ but also on the type of the NOs: For an electron pair bond, a bonding orbital and an antibonding orbital are identified and are given a special treatment. This requires preselection of NOs of a specific type, which is inconvenient in calculation and can even cause problems, when the type of a relevant NO changes during dissociation. In a functional for general use such special orbitals should be distinguished by their occupation numbers, which should be feasible given the well-known fact that upon dissociation these orbitals acquire occupations tending to 1.0 from above (for the bonding orbital) and from below (for the antibonding orbital). In general, strong correlation effects causing occupation numbers to differ significantly from 2.0 and 0.0 should be treated automatically and effectively.

In this paper a DMFT functional is proposed with a fully automatic occupation number driven determination of the (approximate) matrix elements of the two-matrix cumulant. In Sec. II the earlier introduced repulsive corrections, culminating in $C3$, are characterized and the automatic incorporation of these corrections ($AC3$), leading to an expression for the c_{ij} of the form

$$c_{ij}^{AC3}(n_i,n_j) = [1 - D_{ij}(n_i,n_j)]c_{ij}^{(2)}(n_i,n_j), \tag{1.9}$$

is presented. In Eq. (1.9) $D_{ij} \geq 0$ is a parametrized damping function, which assures that c^{AC3} is reduced compared to the two-electron $c^{(2)}$ of Eq. (1.7), when appropriate. Unlike $C3$, the proposed $AC3$ does not require the manual selection of the bonding and antibonding NOs of a bond. Instead, the c_{ij}^{AC3} are automatically determined, based only on the values of n_i and n_j, during self-consistent DMFT calculations. In Sec. III the results of comparative PNOF0, ML, and $AC3$ calculations of the potential curves for the dissociating electron pair bond X-H are presented for the series of the ten-electron hydrides CH_4, NH_3, H_2O, and HF as well as for the molecules H_2 and HCN. $AC3$ reproduces well the reference potential curves of the multireference configuration interaction (MRCI) method for all interatomic distances X-H in the ten-electron series and HCN. In H_2 it has a spurious maximum in the curve at ca. 4 bohr, but it delivers the correct dissociation limit. PNOF0 and ML perform well close to R_e, but the *E versus R* curves go considerably too high at large R, i.e., these functionals seriously underestimate the stability of the molecules when the strong nondynamical correlation occurs that is characteristic of the dissociation (weak bonding) region. In Sec. IV the conclusions are drawn.

II. THE CORRECTIONS UP TO *C*3 AND THE AUTOMATIC INCORPORATION BY *AC*3

Reference 20 as a first step introduced the $C1$ correction to the $\sqrt{n}$ functional of Eq. (1.8), which restores the positive phase f_{ij} of the cross products between different weakly occupied NOs ($i,j \neq i > N/2$) in Eq. (1.6) as it appears in the two-electron cumulant [Eq. (1.7)]. With this, $C1$ employs just that two-electron cumulant, which performs well for the prototypical two-electron systems in the case of dynamical correlation (high Z two-electron ions) as well as nondynamical correlation (dissociating two-electron bond),

$$c_{ij}^{C1}(n_i,n_j) = c_{ij}^{(2)}(n_i,n_j). \tag{2.1}$$

This implies that $D^{C1}=0$. The other repulsive corrections are applied on top of $C1$, and therefore can take the form [Eq. (1.9)] of a damping of the two-electron coefficients $c_{ij}^{(2)}$. The second correction $C2$ eliminates the $c_{ij}^{(2)}$ between different strongly occupied NOs ($i,j(\neq i) \leq N/2$), which amounts to reverting to just normal exchange terms and no corrections employing $\sqrt{n_i n_j}$, i.e., $c_{ij}=0$ for those NO pairs,

$$c_{ij}^{C2}(n_i,n_j) = \begin{cases} 0, & i,j(\neq i) \leq N/2 \\ c_{ij}^{(2)}(n_i,n_j), & \text{otherwise} \end{cases} \quad \text{or} \quad \begin{cases} D_{ij}^{C2} = 1, & i,j(\neq i) \leq N/2 \\ D_{ij}^{C2} = 0, & \text{otherwise}. \end{cases} \tag{2.2}$$

Henceforth, we will simply denote the strongly occupied NOs ($i \leq N/2$) as "occupied orbitals" and the weakly occupied NOs ($i > N/2$) as "virtual" or "unoccupied orbitals." Note that Eq. (2.2) describes, different from Ref. 20, the $C2$ correction *including* the $C1$ correction, in the same way the $C3$ correction as defined below now comprises $C1$ and $C2$.

In the third step ($C3$), considered in the case of a σ-bonded molecule, the $C2$-type correction for off-diagonal occupied i,j terms is applied also to the products of the virtual antibonding NO χ_a of the σ-bond with all strongly occupied NOs, except the bonding NO χ_b. This requires selection of the antibonding orbital χ_a from among the virtuals and exclusion of the bonding orbital χ_b from the set of the occupied NOs $\{\chi_i\}$ so that all $c_{ai}^{(2)}$ and $c_{ia}^{(2)}$ ($i(\neq b) \leq N/2$) can

be eliminated ($D_{ai}=D_{ia}=1$). Furthermore, the $C2$ correction of using full exchange-type terms for off-diagonal occupied orbitals (elimination of c_{ij}, $i,j(\neq i)\leq N/2$) is now extended to *all* diagonal (virtual and occupied) coefficients c_{ii}, except those with $i=a,b$. This implies that the $i=j$ terms in the exchange energy will have the same prefactor $(1/2)n_i n_i$ as the diagonal terms in the Coulomb energy, but with minus sign, and therefore will cancel those. [This is not a self-interaction elimination, that is only the case when all n_i are 0 or 2 as in Hartree–Fock.] This "diagonal" correction has been applied by GU,[9] but it has been demonstrated that its application to the bonding and antibonding pair of orbitals leads to large errors at long distance.[20,28] The c_{ij}^{C3} assume the form

$$c_{ij}^{C3}(n_i,n_j)=\begin{cases}0, & i,j(\neq i)\leq N/2\\ 0, & i=a,j\leq N/2;j=a,i\leq N/2\\ 0, & i=j(\neq a,\neq b)\\ c_{ij}^{(2)}(n_i,n_j), & \text{otherwise}\end{cases}\quad \text{or}\quad \begin{cases}D_{ij}^{C3}=1, & i,j(\neq i)\leq N/2\quad (C2\ \text{correction})\\ D_{ij}^{C3}=1, & i=a,j(\neq b)\leq N/2;j=a,i(\neq b)\leq N/2\\ D_{ij}^{C3}=1, & i=j(\neq a,\neq b)\\ D_{ij}^{C3}=0, & \text{otherwise}.\end{cases} \tag{2.3}$$

It is a disadvantage of this selective application of "off-diagonal" and diagonal corrections that, in order to use Eq. (2.3), one has to select the bonding and antibonding NOs prior to calculation. Furthermore, the $C3$ correction might break the smoothness of the potential energy curve when the bonding character of NOs changes during dissociation. Moreover, the singling out of the bonding-antibonding pair of orbitals should be generalized to special treatment of any strong correlation, manifesting itself in occupation numbers differing strongly from 2.0 and 0.0 (even tending to 1.0 from above or below).

In order to apply all the strong-correlation types of corrections in an automatic fashion within $AC3$, we propose to determine the coefficients c_{ij} by starting with the basic cumulant $c_{ij}^{(2)}$ of the two-electron model, according to $C1$, and apply the further corrections in a continuous fashion with the damping $[1-D_{ij}(n_i,n_j)]c_{ij}^{(2)}(n_i,n_j)$ of $c_{ij}^{(2)}$. To accomplish this, we use the damping function D_{ij} with the following parametrized damping factors $D_d(x)$ and $D_o(x)$ for diagonal terms $(x=n_i-1)$ and off-diagonal terms $(x=n_i+n_j-2)$, respectively,

$$\begin{aligned}D_{ij}(n_i,n_j)=&(1-\delta_{ij})\theta(N/2-i)\theta(N/2-j)+\delta_{ij}D_d(n_i-1)\\&+\{\theta(N/2-i)[1-\theta(N/2-j)]\\&+\theta(N/2-j)[1-\theta(N/2-i)]\}D_o(n_i+n_j-2),\end{aligned} \tag{2.4}$$

where D_d and D_o are the following rational functions (Padé approximants):

$$D_{d/o}(x)=\frac{P_{d/o}^2(x)}{1+P_{d/o}^2(x)}, \tag{2.5}$$

$$P_{d/o}(x)=a_{d/o}x^2(x^2-2), \tag{2.6}$$

and $\theta(x)$ is the Heaviside step function [here we define $\theta(0)=1$]. These functions are zero around $x=0.0$ and they approach a constant for $x=\pm 1$, see Fig. 1 for these functions after the parameter optimization discussed below. The first term in D_{ij} is the $C2$ correction, i.e., elimination $(D_{ij}=1)$ of the off-diagonal $(1-\delta_{ij})$ occupied-occupied $(\theta(N/2-i)\theta(N/2-j))$ cumulant $c_{ij}^{(2)}$, see Eq. (2.2). The second term, with damping function $\delta_{ij}D_d(n_i-1)$, takes care of the $C3$ correction for the diagonal terms [third entry in Eq. (2.3)], where $(1-D_d)$ [in Eq. (1.9)] should effect damping of the $c_{ii}^{(2)}$ except for the bonding and antibonding orbitals or in general when the occupation numbers approach 1.0. This can be achieved with a function D_d obeying $D_d\approx 1$ when $n_i\approx 0$ or $n_i\approx 2$, i.e., $x=n_i-1\approx\pm 1$, and $D_d\approx 0$ when $n_i-1\approx 0$. The third term in Eq. (2.4) applies the remaining $C3$ correction [second entry of Eq. (2.3)], i.e., damping in the cumulant of the $c_{ia}^{(2)}$ and $c_{ai}^{(2)}$ off-diagonal coefficients with the factor $(1-D_o)$ [in Eq. (1.9)] for the cross terms between the antibonding orbital a with occupied orbitals $i\leq N/2$, except when i is the bonding orbital, $i=b$. In expression (2.4) the θ functions switch this D_o term on for (ij) an occupied-virtual pair or a virtual-occupied pair. We need two further restrictions: (a) among the virtual orbitals only the antibonding orbital (the virtual orbital with significant population $n_i\uparrow 1.0$) should be selected and (b) among the occupied orbitals the bonding partner of a [the occupied orbital with occupation significantly different from 2.0, $n_i\downarrow 1.0$)] should be ex-

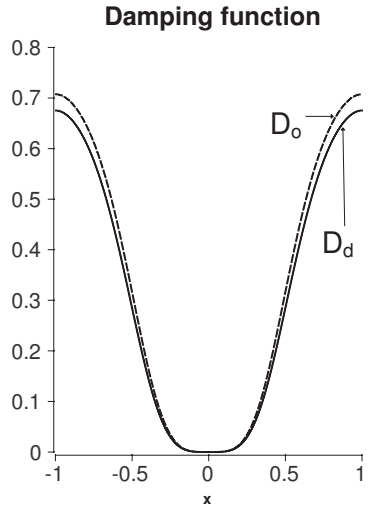

FIG. 1. The $AC3$ damping functions (a) $D_d(n_i-1)$ and (b) $D_o(n_i+n_j-2)$.

cluded. These restrictions are simultaneously effected with the function $D_o(n_i+n_j-2)$: (*a*) antibonding-occupied pairs: When $n_i \approx 1$ and $n_j \approx 2$, or $n_j \approx 1$ and $n_i \approx 2$, $D_o(x \approx 1.0) \approx 1$, full damping; (*b*) other virtual-occupied pairs: When $n_i \approx 0$ and $n_j \approx 2$, or $n_j \approx 0$ and $n_i \approx 2$, $D_o(x \approx 0.0) \approx 0$, no damping and full $c_{ij}^{(2)}$; (*c*) antibonding-bonding pair: If both n_i and n_j are close to 1, $x=n_i+n_j-2 \approx 0$ and $D_o=0.0$, no damping and full $c_{ij}^{(2)}$.

The optimal parameters $a_d=1.4423$ and $a_o=1.5552$ in D_d and D_o are chosen to reproduce the MRCI energies of the molecules HF and H_2O at the equilibrium geometry and also when one bond is stretched at $R(\mathrm{F-H})=4.0$ and $R(\mathrm{O-H})=5.0$ bohr. These are very few fitting points, but they already yield satisfactory results. The parameters are generated, initially, with a nonlinear numerical optimization by the downhill simplex method and their refinement was carried out with the gradient quasi-Newton method of Broyden–Fletcher–Goldfarb–Shanno. Figure 1 displays the functions $D_{d/o}$ calculated with these parameters. Due to the similar values of a_d and a_o, the functions $D_d(x)$ and $D_o(x)$ are rather close to each other, displaying only a clear difference near the end points $x=\pm 1$ (see Fig. 1). We have tested the use of a single averaged parameter. As a rule, *AC*3 with different a_d and a_o yields somewhat better results compared to those with a single averaged parameter $a=a_{d/o}$, so that in Sec. III results with two parameters will be presented.

An important feature of the present *AC*3 is that, just as the initial $\sqrt{n}$ functional and its *C*1–*C*3 corrections, *AC*3 incorporates the asymptotically correct Heitler–London description of a dissociating single bond (the dissociating H_2 molecule) when the occupations n_b and n_a of the bonding and antibonding NOs tend to each other, $n_b \approx n_a \approx 1$.[11] Indeed, by construction, the functions D_d and D_o reach their minima at $n_i=1$ and $n_i+n_j=2$, respectively, with both minima being zero, $D_{d/o}(0)=0$ (see Fig. 1). This means that the *AC*3 cumulant [Eq. (1.9)] correctly turns to the paradigmatic $c_{ij}^{(2)}$ of the two-electron system, Eq. (1.7), in this case. Furthermore, with $D_o(0)=0$ the cumulant $c_{ij}^{(2)}$ is also retained in the important case of dynamical correlation, which is represented with interaction between the strongly occupied NOs χ_i with $n_i \approx 2$ and weakly occupied NOs χ_j with $n_j \approx 0$. We note that the value of the optimized function D_d in the end points $x=\pm 1$ is not 1.0 but 0.64 (see Fig. 1), so the diagonal part of the *C*3 correction [third entry of Eq. (2.3)] is not fully in effect. The $c_{ii}^{(2)}$ coefficient in the cumulant for both weakly occupied NOs χ_i with $n_i \approx 0$ and for strongly occupied core and deep valence NOs χ_i with $n_i \approx 2$ is not completely eliminated but is reduced to ca. 36%. In turn, the off-diagonal part of the *AC*3 correction, governed by the function D_o with $D_o(\pm 1)=0.71$ (see Fig. 1), reduces in the cumulant $c_{ai}^{(2)}$ coefficients between the antibonding NO χ_a with $n_a \approx 1$ and the strongly occupied NOs χ_i with $n_i \approx 2$ by a factor of 0.29 instead of eliminating them as in the original *C*3 correction.

Figure 2 compares the *AC*3 and the BBC3 potential energy curves for the HF molecule with the reference MRCI one (see Sec. III for the computational details). *AC*3 yields consistently higher energies than BBC3 and on average it improves the agreement between DMFT and MRCI, which is especially true in the dissociation region of 4–5 bohr (see Fig. 2). A possible reason for this latter improvement is that a relatively high value $D_o(-1)=0.71$ reduces the cumulant $c_{bj}^{(2)}$ coefficients between the bonding NO χ_b with $n_b \approx 1$ and weakly occupied NOs χ_j with $n_j \approx 0$ in *AC*3, while in the original BBC3 the full $c_{bj}^{(2)}$ is retained in this case.

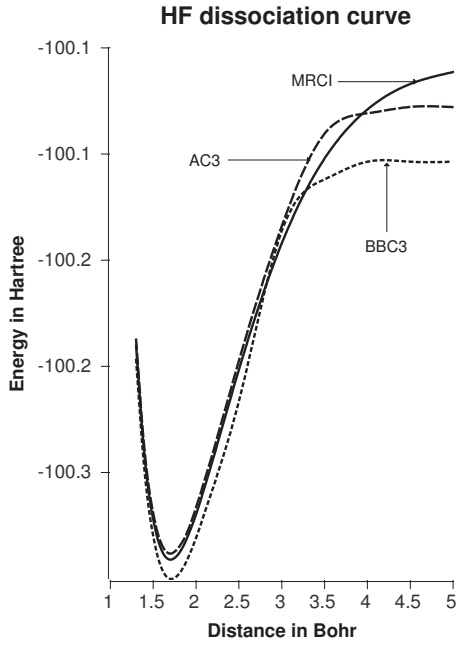

FIG. 2. Energy curves for the molecule HF calculated with the DMFT functionals BBC3, *AC*3, and with the MRCI method.

The *AC*3 modulation of the $c_{ij}^{(2)}$ form of the cumulant depends only on the magnitude of the NO occupations and removes the explicit dependence of the *C*3 correction [Eq. (2.3)] of c_{ij} on the type of NOs, thus permitting automatic calculation of c_{ij}^{AC3} within the self-consistent DMFT procedure. The results of test calculations with the *AC*3 functional will be presented in Sec. III.

III. COMPARATIVE *AC*3 calculations of the potential energy curves

In this section the results of comparative calculations of the potential energy curves with the approximate DMFT functionals PNOF0, ML, and *AC*3 are presented. The cumulant of PNOF0 can be represented in the form

$$c_{ij}^{\mathrm{PNOF0}}(n_i,n_j)=[1-\delta_{ij}]c_{ij}^{(2)}(n_i,n_j). \tag{3.1}$$

It uses the full $c_{ij}^{(2)}$ (correction *C*1 to the $\sqrt{n}$ functional), except that all diagonal terms are omitted from the cumulant, implying that the diagonal terms in the Coulomb energy and the exchange energy cancel (the full diagonal GU correction). In turn, the ML cumulant has the following form:

$$c_{ij}^{\mathrm{ML}}(n_i,n_j)=\frac{1}{2}n_in_j-\frac{1}{2}n_in_j\frac{a_0+a_1n_in_j}{1+b_1n_in_j}. \tag{3.2}$$

The factor (1/2) in the second term, which is missing in the ML paper,[32] arises because we use summation over orbitals, not spin orbitals, and have occupation numbers ranging from 0.0 to 2.0, not 0.0 to 1.0 as Marques and Lathiotakis[32] used. The ML functional has been introduced as a fully empirical form, with a_0 resulting from the condi-

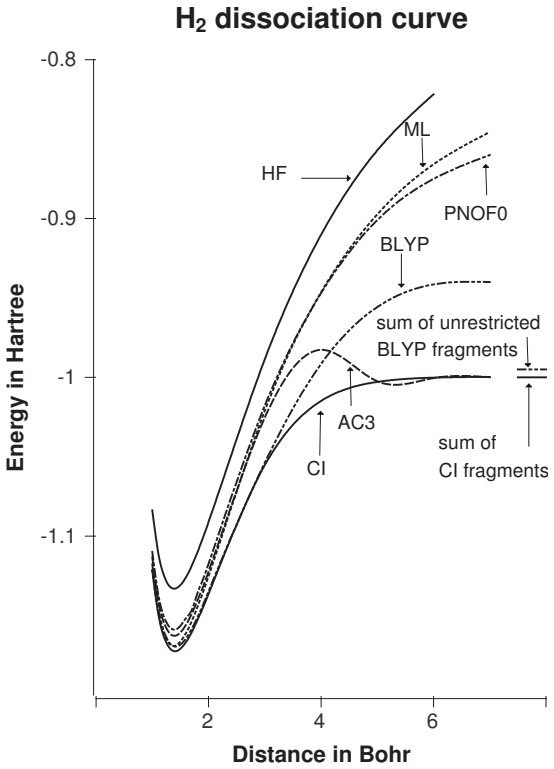

FIG. 3. Energy curves for the molecule H_2 calculated with the DMFT functionals ML, PNOF0, *AC*3, DFT functional BLYP, and HF and FCI methods. The levels in the right-hand side mark the sum of the energies of two individual H atoms calculated with unrestricted BLYP, unrestricted HF and MRCI.

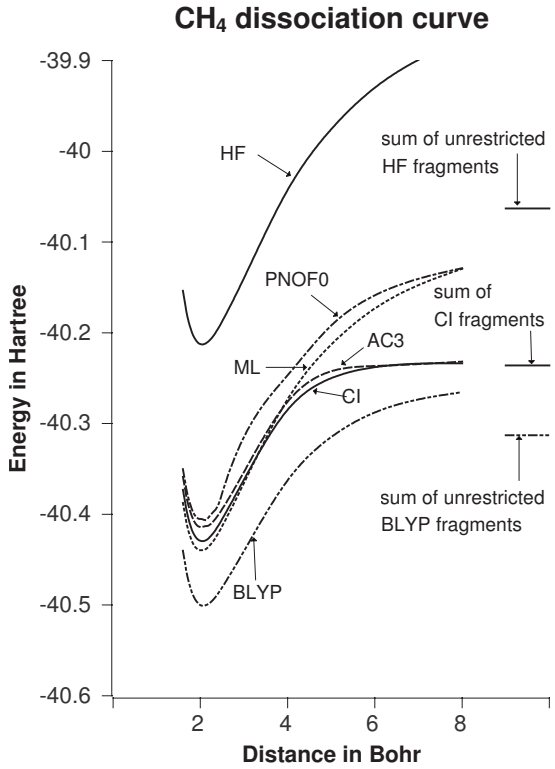

FIG. 4. Energy curves for dissociation of a single C–H bond of CH_4, keeping the geometry of the CH_3 fragment fixed. Calculations with the DMFT functionals ML, PNOF0, *AC*3, DFT functional BLYP, and HF and MRCI methods. The levels in the right-hand side mark the sum of the energies of the individual fragments H and CH_3 calculated with unrestricted BLYP, unrestricted HF and MRCI.

tion that the Hartree–Fock limit is recovered and the parameters a_1 and b_1 are fitted to reproduce the energies E_c of a series of prototype molecules calculated in the 6-13G* basis at the equilibrium geometry.[32]

Figures 3–8 display the PNOF0, ML, and *AC*3 potential energy curves for the dissociation of the electron pair bond $X-H$ in H_2, in the series of the ten-electron hydrides CH_4, NH_3, H_2O, and HF as well as in HCN. The type of the bonds calculated ranges from the covalent electron pair bonds H–H and C–H to the strongly polar bonds O–H and F–H. The DMFT-*AC*3 calculations are performed according to the procedures in Refs. 33 and 34. A minimum is found in an iterative process, each iteration consisting of two steps: the NOs are optimized (again iteratively) with fixed occupation numbers and then the occupation numbers are optimized. The occupation number optimizations are fast, but the NO optimization is relatively slow, scaling as M^5 if M is the basis set size. The $\sqrt{n}$ functional, using only J and K integrals, leads to computational expense similar to Hartree–Fock. The corrections that are added, however, use specific integrals over the NOs, making four-index transformations necessary. For a correlated method the scaling is still quite acceptable.

The reference curves are those of the full CI (FCI) for H_2 and of MRCI for the other molecules calculated with the GAMESS-U.K. package.[35] As a natural reference, the curves of the restricted HF method are also included as well as those of the standard functional of Becke–Lee–Yang–Parr (BLYP)[36,37] of DFT. For the DFT-BLYP calculations the DALTON package[38] is employed. Calculations are performed in the correlation-consistent polarized cc-*p*VTZ basis set for all atoms.[39] For heavier atoms C, N, O, and F, the *f*-function and the most diffuse *d*-function are excluded from the basis. Since our primary goal is comparative calculations, the geometry of the dehydrogenated fragments is not optimized during dissociation and they are kept frozen at the equilibrium geometry of the intact molecule.

Figures 3–8 demonstrate a large difference between the reference FCI/MRCI curves and the restricted HF ones. This reflects the well-known HF error of too high (not sufficiently negative) electronic energies due to its neglect of electron correlation. This error increases significantly in the dissociation limit. It is somewhat less well known that the potential curves of the spin-restricted standard DFT functionals exhibit a similar dissociation limit deficiency,[24] as can be clearly seen in Fig. 3 for H_2. In this case BLYP reproduces the FCI curve near the equilibrium geometry, while at larger interatomic distances $R(H-H)$ it makes the same qualitative error as HF. Although not to the same extent as HF, BLYP still substantially underestimates the strong nondynamical left-right correlation in dissociating H_2. Clearly, the picture behind standard DFT functionals of an xc hole localized around the reference electron, which is fundamentally right if the reference electron is near one nucleus in the stretched H_2 system, still cannot take into account that the left-right correlation pushes the other electron as far away as the other remote nucleus of the dissociating H_2.[24] This left-right correlation error of generalized gradient approximation-DFT

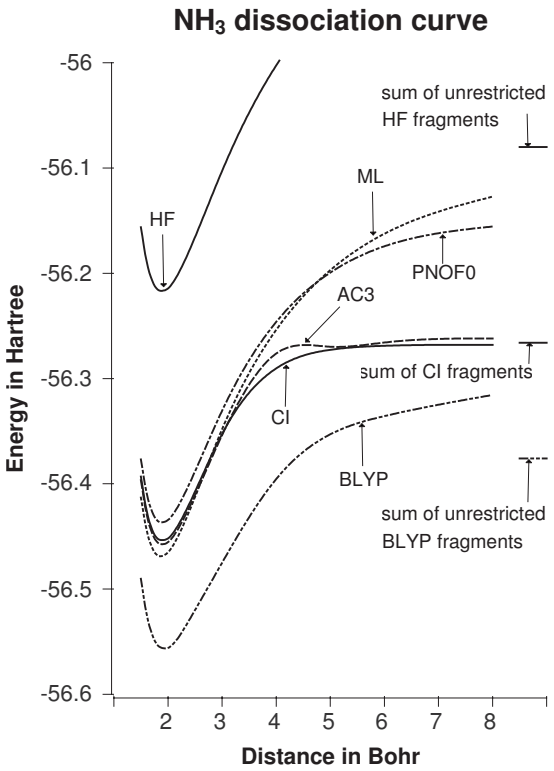

FIG. 5. Energy curves for the dissociation of a single N–H bond of the molecule NH_3, keeping the geometry of the NH_2 fragment fixed. Calculations with the DMFT functionals ML, PNOF0, *AC*3, DFT functional BLYP, and HF and MRCI methods. The levels in the right-hand side mark the sum of the energies of the individual fragments H and NH_2 calculated with unrestricted BLYP, unrestricted HF and MRCI.

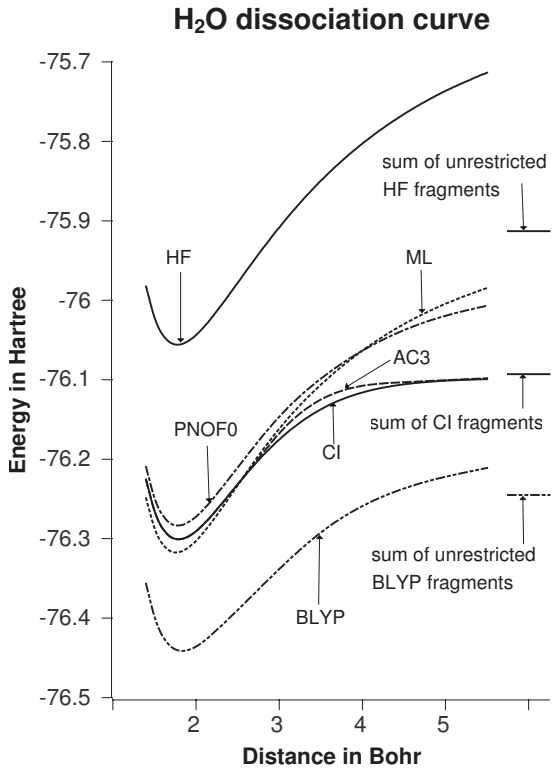

FIG. 6. Energy curves for the dissociation of a single O–H bond of the molecule H_2O, keeping the geometry of the OH fragment fixed. Calculations with the DMFT functionals ML, PNOF0, *AC*3, DFT functional BLYP, HF and MRCI methods. The levels in the right-hand side mark the sum of the energies of the individual fragments H and OH calculated with unrestricted BLYP, unrestricted HF and MRCI.

(BLYP) for H_2 can be estimated from the difference between the energy E^{BLYP}(restricted) of the dissociated molecule calculated with the spin-restricted BLYP and the sum $E_{\mathrm{frag}}^{\mathrm{BLYP}}$(unrestricted) of the energies of open-shell fragments calculated with the spin-unrestricted BLYP and depicted in Figs. 3–7. In H_2 we have the special case that the restricted BLYP energy is close to the FCI energy at R_e, and the spin-unrestricted BLYP energy of the H fragment is again close to the accurate energy of the H atom, so the difference between the asymptotic restricted BLYP energy and the asymptotic FCI energy is just the left-right correlation error of BLYP. When BLYP is not close to the MRCI energy, as is the case for the other molecules, both at R_e for the restricted BLYP and asymptotically for unrestricted BLYP, the BLYP left-right correlation error follows just from the difference of asymptotic restricted BLYP calculation of the molecule and the unrestricted BLYP calculations on the fragments.

A well-known feature of CI is the strong dependence of its results on the basis set. For the two-electron H_2 the CI calculations in the chosen basis produce results, which are close to the basis set limit. However, for the ten-electron systems the present basis is a rather moderate one, although it is already one of the largest basis sets used in DMFT calculations. In turn, the DFT results are less basis set dependent. The absolute value of the total DFT energy (with an approximate functional) does not have the exact total energy as a lower bound, and the functionals are usually parametrized (as the BLYP used here) to effectively account for the dynamical electron correlation in atoms. Because of this, the BLYP curves for the ten-electron series go substantially lower than the reference MRCI ones (see Figs. 4–7) over the whole R range, including the asymptotic region. This does not mean much. The performance of the DFT functionals is usually not judged by the total energies but just by the difference between atomic and molecular energies. In these cases (Figs. 4–7) the asymptotic restricted BLYP error, as mentioned, cannot be judged from the difference between restricted BLYP and MRCI at the end point, but can be estimated from the difference between the end point of the restricted BLYP potential curve and the unrestricted $E_{\mathrm{frag}}^{\mathrm{BLYP}}$ energy. In all cases the spin-restricted BLYP produces an appreciable left-right correlation error, although it is usually somewhat smaller than the abovementioned error in the case of H_2 (however, the limiting value on the restricted BLYP curve has not always been reached in the figures).

An interesting finding of this paper is that, just as restricted HF and restricted BLYP, the DMFT functionals PNOF0 and ML consistently underestimate the relative stability of stretched molecules. Due to this, the PNOF0 and ML curves exhibit much larger deviations from the FCI/MRCI curves in the dissociation region, while near equilibrium they go relatively closer to FCI/MRCI (see Figs. 3–8). For the dissociating H_2 the PNOF0 error and the (larger) ML error are both rather close to the large HF error. Also for the ten-electron hydrides and HCN, the upward shift of the PNOF0 and ML curves in the dissociation region is clear,

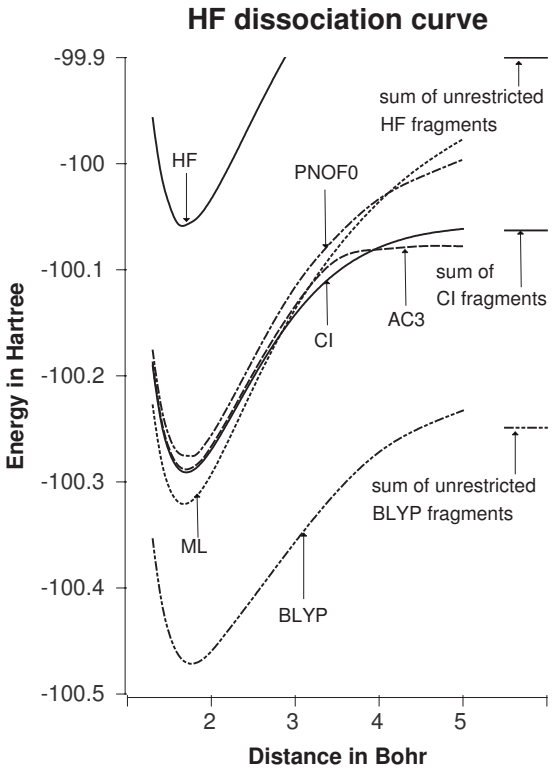

FIG. 7. Energy curves for the molecule HF calculated with the DMFT functionals ML, PNOF0, *AC*3, DFT functional BLYP, and the HF and MRCI methods. The levels in the right-hand side mark the sum of the energies of the individual atoms H and F calculated with unrestricted BLYP, unrestricted HF and MRCI.

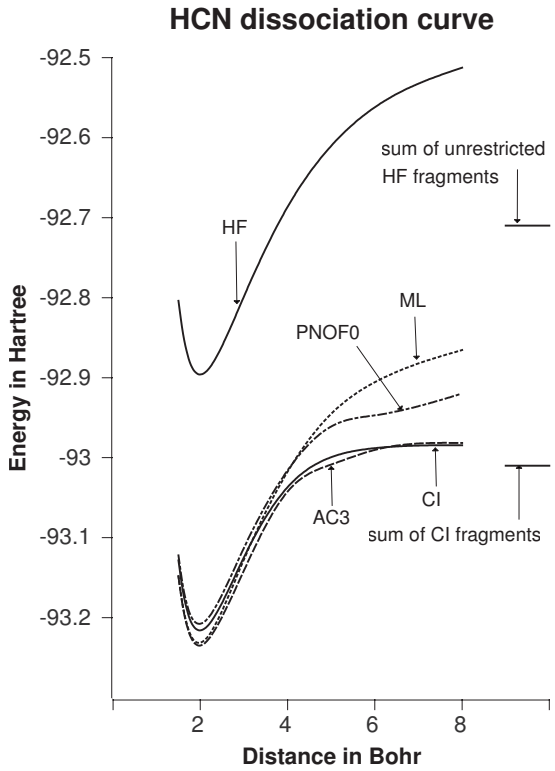

FIG. 8. Energy curves for the dissociation of the H–C bond of the molecule HCN, keeping the geometry of CN fixed. Calculation with the DMFT functionals ML, PNOF0, *AC*3, and the HF and MRCI methods. The levels in the right-hand side mark the sum of the energies of individual fragments H and CN calculated with unrestricted HF and MRCI.

and the corresponding absolute deviations remain large (see Figs. 4–8). For the largest distances in the figures (which correspond to the asymptotic energies for MRCI and *AC*3, but clearly do not yet represent the dissociation limit for BLYP, PNOF0, and ML curves) the lower bound to the ML error ranges from ca. 0.1 hartree for HF and CH_4 to 0.14 hartree for NH_3, while the somewhat smaller (lower bound to the) PNOF0 error ranges from 0.07 hartree for HCN to 0.1 hartree for NH_3. In the case of PNOF0 the asymptotic error originates from the disregard in this functional of the strong-correlation situations, where NO occupations may tend to 1.0. The PNOF0 functional applies out of the set of *C*3 corrections only the third entry in Eq. (2.3) but without the precaution of *C*3 of excluding from that correction the orbitals with occupations tending to 1.0 (the "bonding" and "antibonding" ones). This implies application of the full diagonal GU correction, which results in the neglect of the diagonal two-electron cumulant $c_{ii}^{(2)}$ throughout, also for the bonding and antibonding NOs. As was argued in Ref. 20, this neglect destroys the asymptotically correct Heitler–London description of the left-right correlation and it leads to a substantial underestimation of stability of the dissociating molecules.

The ML functional is a total modification of the $\sqrt{n}$ functional. The $(1/2)n_in_j$ term in Eq. (3.2) cancels the exchange term in Eq. (1.5), and the whole exchange-correlation energy is then represented with the second term in Eq. (3.2) replacing $-\sqrt{n_in_j}$. The parameter optimization for the ML functional used the equilibrium geometries of a subset of the *G*2 set of molecules, and therefore did not probe strong correlation cases with occupation numbers close to 1.0. In the systems with only dynamical correlation (closed shell molecules at R_e) studied by ML, only occupation number ranges occur close to 2.0 (or 1.0 in the scale 0.0–1.0 used by ML) and close to 0.0, see Fig. 2 of Ref. 32. The ML functional achieves very good correlation energies at R_e for molecules with these occupation number ranges. For high occupation numbers the ML functional is smaller than the $\sqrt{n}$ functional, leading to less negative energies. The same effect is achieved with the *C*2 correction, see discussion in Ref. 20 for the effect of this correction for the strongly occupied orbitals. For small occupation numbers the ML functional for most of the n_in_j values that occur appears to be larger than the $\sqrt{n}$ functional (more stabilizing). The empirical parameter fitting obviously is able to strike a good balance between these positive and negative effects, so that the net effect is less stabilized than the (overcorrelating) $\sqrt{n}$ functional. However, the ML functional appears to fall short of the $-\sqrt{n_in_j}K_{ij} \approx -K_{ij}$ stabilizing contribution, which is appropriate in the dissociation limit when $n_i \approx n_j \approx 1.0$. At this point the ML functional, being in that region linear in $(1/2)n_in_j$, see Fig. 1 of Ref. 32, obtains only $-(1/2)K_{ij}$. This error is made for the diagonal terms with c_{ii}^{ML}, $i=a,b$, and the off-diagonal c_{ab}^{ML} term. This is presumably the reason that the energy of the ML curves goes rather too high (not stabilizing enough) in the dissociation region. So it appears that it is the neglect of the strong nondynamical correlation situations in both the ML and PNOF0 functionals that leads to the large errors of these functionals at long bond distances.

TABLE I. Comparison of the ML, PNOF0, and *AC*3 and MRCI total E_{tot} and correlation E_c energies (in a.u.) for the equilibrium geometry.

	H_2	CH_4	NH_3	H_2O	HF	HCN
HF						
E_{tot}	−1.133	−40.213	−56.216	−76.055	−100.056	−92.896
CI						
E_{tot}	−1.172	−40.430	−56.453	−76.301	−100.291	−93.216
E_c	−0.039	−0.217	−0.237	−0.246	−0.235	−0.320
*AC*3						
E_{tot}	−1.163	−40.414	−56.457	−76.301	−100.288	−93.235
E_c	−0.030	−0.201	−0.241	−0.246	−0.232	−0.339
Error (%)	23.1	7.4	−1.7	0.0	1.3	−5.9
ML						
E_{tot}	−1.169	−40.439	−56.468	−76.316	−100.320	−93.231
E_c	−0.036	−0.226	−0.252	−0.261	−0.264	−0.335
Error (%)	7.7	−4.1	−6.3	−6.1	−12.3	−4.7
*PNOF*0						
E_{tot}	−1.156	−40.406	−56.437	−76.283	−100.276	−93.208
E_c	−0.023	−0.193	−0.221	−0.228	−0.220	−0.312
Error (%)	41	11.1	6.8	7.3	6.4	2.8

BBC3 and *AC*3 have been constructed with the aim to yield good correlation energies also in regions where interactions between atoms become weak and the (nondynamical) correlation becomes large. It is gratifying that the *AC*3 curves are fulfilling the expectations. The *AC*3 reproduces well the full reference MRCI potential curves for the ten-electron series and HCN (see Figs. 4–8). The best *AC*3 case appears to be H_2O, for which the *AC*3 curve coincides (on the scale in Fig. 6) with the MRCI one both around the equilibrium distance and in the dissociation limit, while the only visible discrepancy between the curves occurs in the intermediate region 3 bohr$<R$(O–H)<5 bohr. This trend holds also for other ten-electron hydrides and HCN. There is, however, a serious deficiency in the curve for H_2. Around 3.75 bohr there is a spurious maximum in the *AC*3 curve, and at distances larger than 2 bohr it already starts to deviate considerably from the FCI curve. It is actually rather close between 2 and 3 bohr to the PNOF0 and ML curves, but it turns down to the correct asymptotic behavior too late, so the mentioned maximum appears. This behavior is most extreme in the case of H_2 but is also exhibited by most other curves. It is possibly due to the symmetric form of the damping factors D_d and D_o, and further optimization of the *AC*3 functional will need to address this point by considering more flexible, possibly asymmetrical, damping factors.

Considering now the behavior of the various functionals around R_e, we note that in this small sample of molecules *AC*3 appears to be closest to the reference MRCI curves: for the ten-electron hydrides the PNOF0 and ML curves appear to bracket the *AC*3 curve, PNOF0 being too high and ML too low for CH_4, H_2O, NH_3, and HF. At R_e *AC*3 is closest to the benchmark MRCI result for NH_3, H_2O, and HF, but for HCN PNOF0 is the closest, ML and *AC*3 having a very similar slightly larger deviation. HCN is the only case where the *AC*3 shows a small but clear deviation toward stronger bonding with respect to the MRCI curve for a long range of intermediate distances (2.5–6 bohr). In order to quantify the behavior around R_e somewhat better, we present in Table I the DMFT and FCI/MRCI total energies E_{tot} and correlation energies E_c calculated at the equilibrium geometry. H_2 is special; it is the only case where all DMFT functionals appreciably underestimate the correlation, for *AC*3 and PNOF0 with large percentages (23% and 41%, respectively). In all many-electron systems the errors are small. For the ten-electron hydrides and HCN, ML consistently overestimates correlation and PNOF0 consistently underestimates it, while *AC*3 produces errors of either sign, with the average absolute error of *AC*3 (3.3%) being about twice as small as the ML (6.7%) and PNOF0 (6.9%) errors. Since our set of molecules is small, we can only draw a very tentative conclusion from this comparison. It is notable that the extensive benchmarking performed by Lathiotakis and Marques in Ref. 31, which did not yet include the ML functional, yielded very similar quality for the BBC3 and PNOF0 functionals. Very recently, Marques and Lathiotakis[32] showed that the ML functional performed, on average, better for the correlation energies at R_e over the *G*2 set. The average error of 3.3% in our small sample is lower than either the ML result (11%) or the BBC3 result (18%) in Ref. 32 over the whole *G*2 set. This may just be accidental; it may also be due to the fact that we use larger basis sets or the *AC*3 results may be a bit better than the BBC3 functional tested by Marques and Lathiotakis.[32]

Table II compares the equilibrium bond distances $R_e(X-H)$ calculated with the HF, FCI/MRCI, ML, PNOF0, *AC*3, and BLYP with the corresponding experimental values. Among the reference methods, HF produces the shortest bonds in all cases (except for CH_4 and HCN). CI yields, on average, longer bonds, while the experimental R_e values are still larger and BLYP produces the longest bonds, typically 0.01–0.03 bohr longer than experiment. Among the DMFT functionals, ML produces the shortest bonds, while *AC*3 yields the best correspondence with CI. Indeed, for H_2O and

TABLE II. Comparison of the calculated equilibrium bond distances (in a.u.).

	H_2	CH_4	NH_3	H_2O	HF	HCN
HF	1.388	2.044	1.888	1.777	1.694	1.995
CI	1.403	2.042	1.896	1.789	1.704	1.989
*AC*3	1.390	2.045	1.897	1.789	1.704	1.978
ML	1.378	2.019	1.868	1.759	1.674	1.967
PNOF0	1.385	2.030	1.890	1.782	1.714	1.975
BLYP	1.411	2.068	1.931	1.835	1.764	
Experiment	1.401	2.050	1.912	1.809	1.733	2.010

HF, *AC*3 reproduces the CI R_e values with all three digits, while for NH_3 the corresponding difference is only 0.001 bohr (see Table II).

IV. CONCLUSIONS

In this paper a one-electron density matrix functional is proposed, which employs only J and K integrals with an automatic (occupation number driven) calculation of the expressions for the $\Gamma_{xc,ijji}$ elements of the exchange-correlation part of the two-matrix, which lead to exchangelike matrix elements. The form of the exchange-correlation part of the new functional reads

$$E_{xc}^{AC3}[\gamma] = -\frac{1}{4}\sum_{ij} n_i n_j K_{ij} + \frac{1}{2}\sum_{ij} [1 - D_{ij}(n_i,n_j)]c_{ij}^{(2)} \times (n_i,n_j)K_{ij},$$

where the functions D_{ij} and $c_{ij}^{(2)}$ are defined in Eqs. (1.7) and (2.4)–(2.6), respectively.

Previously, in the BBC3 functional, the effects of strong (nondynamical) correlation were taken care of by selecting manually the NOs involved in the strong correlation (having occupations tending to 1.0). We have presented this functional in a slightly different way (without changing the physics) by casting it in the form of a modeling of the two-electron cumulant. Since we have based ourselves from the beginning on the so-called *C*1 correction to the $\sqrt{n}$ functional of Eq. (1.8), we effectively start from a functional that is rather accurate for prototypical two-electron cases, Eq. (1.7). While incorporating all the *C*3 corrections to the $\sqrt{n}$ functional,[20] which entered the previously proposed BBC3 functional, *AC*3 has the advantage over the latter that no manual selection of NOs involved in strong correlation (bonding and antibonding NOs in the present case) is required in *AC*3. From the comparisons to other successful functionals we have noted that the proper treatment of strong correlation cases is crucial in order to obtain physically meaningful full potential energy curves. For instance we note that the PNOF0 functional, which uses a subset of the *C*3 corrections but lacks the special treatment of strong correlation included in *AC*3, is almost competitive with *AC*3 around the equilibrium bond length, also for the magnitude of the errors in the correlation energy, but fails to describe the large-*R* region. In the present small sample of molecules the average absolute error of the correlation energies is lowest for *AC*3 (for the ten-electron systems it is only 3.3%). *AC*3 also reproduces very well the equilibrium bond distances for the ten-electron series. For H_2 *AC*3 is free of the large HF and BLYP dissociation limit errors, but the energy curve exhibits a spurious maximum, and the correlation energy is relatively poor (23% error).

One can conclude that *AC*3 correctly reproduces the electron exchange and both dynamical and nondynamical correlation for the investigated systems which, besides the equilibrium or stretched electron pair bond, possess also other unbroken bonds as well as core electrons and electron lone pairs. This has been achieved with *JK*-only functionals of the NOs and the NO occupations. The nonlocality of these functionals, which is inherent in the use of the delocalized NOs, is presumably an important factor in their improvement over pure DFT functionals in the weak interaction region.

The present functional has only two parameters, which have been determined from a very limited number (4) of benchmark calculations. It is remarkable that the *AC*3 functional, without further optimization, achieves similar or even better quality of potential energy curves than its rigid BBC3 predecessor in spite of the fact that the dependence on occupation number and type of orbital is after parameter optimization somewhat different from BBC3. Probably this signifies that there is considerable leeway in the parameter determination. This may turn out to be rather important when further parameter optimization is carried out to improve the H_2 curve along with a larger set of benchmark molecules and covering many more cases of interest (notably multiply bonded systems, open shell systems, transition states, etc.) in a comprehensive density matrix functional. Preliminary *AC*3 calculations of the potential energy curve of the double-bonded C_2H_4 show promising results, while for the triple-bonded N_2 special precautions may be needed to ensure symmetry equivalence (equal occupation numbers!) of the π_x and π_y orbitals, as is effectively done in Ref. 32 in the successful application of BBC3 to multiply bonded systems

We consider it a great advantage of the DMFT functionals that they are very clear in the way that the physics of electron correlation is modeled and which types of correlation are treated. Apart from the dynamical correlation (relevant at R_e for "normal" molecules) and the strong nondynamical correlation at bond breaking, which seem to be amenable by treatment with *JK*-only functionals, van der Waals interactions can also be analyzed and incorporated, although that very different type of correlation would require in principle non-*JK* terms in the cumulant[15] (about half of the van der Waals energy has been obtained with a *JK*-only functional[40]).

ACKNOWLEDGMENTS

One of the authors (O.G.) gratefully acknowledges the support of the Netherlands Foundation for Research (NWO) through its Chemistry Division (Chemische Wetenschappen).

[1] P. O. Löwdin and H. Shull, Phys. Rev. **101**, 1730 (1956).
[2] T. L. Gilbert, Phys. Rev. B **12**, 2111 (1975).
[3] R. A. Donnelly and R. G. Parr, J. Chem. Phys. **69**, 4431 (1978).
[4] M. Levy, Proc. Natl. Acad. Sci. U.S.A. **76**, 6062 (1979).
[5] S. M. Valone, J. Chem. Phys. **73**, 1344 (1980).
[6] A. M. K. Müller, Phys. Lett. **105A**, 446 (1984).
[7] G. Zumbach and K. Maschke, J. Chem. Phys. **82**, 5604 (1985).
[8] M. A. Buijse, Ph.D. thesis, Vrije Universiteit, 1991.
[9] S. Goedecker and C. Umrigar, Phys. Rev. Lett. **81**, 866 (1998).
[10] G. Csanyi and T. A. Arias, Phys. Rev. B **61**, 7348 (2000).
[11] M. A. Buijse and E. J. Baerends, Mol. Phys. **100**, 401 (2002).
[12] J. M. Herbert and J. E. Harriman, J. Chem. Phys. **118**, 10835 (2003).
[13] C. Kollmar and B. Hess, J. Chem. Phys. **120**, 3158 (2004).
[14] K. Pernal and J. Cioslowski, J. Chem. Phys. **120**, 5987 (2004).
[15] O. Gritsenko and E. J. Baerends, J. Chem. Phys. **124**, 054115 (2006).
[16] E. H. Lieb, Phys. Rev. Lett. **46**, 457 (1981).
[17] M. Levy, in *Density Matrices and Density Functionals*, edited by R. Erdahl and V. H. Smith (Reidel, Dordrecht, 1987), p. 479.
[18] L. J. Holleboom, J. G. Snijders, E. J. Baerends, and M. A. Buijse, J. Chem. Phys. **89**, 3638 (1988).
[19] W. Kutzelnigg, J. Chem. Phys. **125**, 171101 (2006).
[20] O. V. Gritsenko, K. Pernal, and E. J. Baerends, J. Chem. Phys. **122**, 204102 (2005).
[21] P. Leiva and M. Piris, J. Chem. Phys. **123**, 214102 (2005).
[22] J. Cioslowski and K. Pernal, Chem. Phys. Lett. **430**, 188 (2006).
[23] E. J. Baerends, Phys. Rev. Lett. **87**, 133004 (2001).
[24] M. Grüning, O. V. Gritsenko, and E. J. Baerends, J. Chem. Phys. **118**, 7183 (2003).
[25] R. L. Frank, E. H. Lieb, R. Seiringer, and H. Siedentop, Phys. Rev. A **76**, 052517 (2007).
[26] E. Cancès and K. Pernal, J. Chem. Phys. **128**, 134108 (2008).
[27] A. J. Cohen and E. J. Baerends, Chem. Phys. Lett. **364**, 409 (2002).
[28] V. N. Staroverov and G. Scuseria, J. Chem. Phys. **117**, 2489 (2002).
[29] J. M. Herbert and J. E. Harriman, Chem. Phys. Lett. **382**, 142 (2003).
[30] M. Piris, Int. J. Quantum Chem. **106**, 1093 (2006).
[31] N. N. Lathiotakis and A. L. Marques, J. Chem. Phys. **128**, 184103 (2008).
[32] M. A. L. Marques and N. N. Lathiotakis, Phys. Rev. A **77**, 032509 (2008).
[33] J. Cioslowski and K. Pernal, J. Chem. Phys. **115**, 5784 (2001).
[34] K. Pernal, Phys. Rev. Lett. **94**, 233002 (2005).
[35] M. F. Guest, I. J. Bush, H. J. J. van Dam, P. Sherwood, J. M. H. Thomas, J. H. van Lenthe, R. W. A. Havenith, and J. Kendrick, Mol. Phys. **103**, 719 (2005).
[36] C. Lee, W. Yang, and R. G. Parr, Phys. Rev. B **37**, 785 (1988).
[37] B. Miehlich, A. Savin, H. Stoll, and H. Preuss, Chem. Phys. Lett. **157**, 200 (1989).
[38] DALTON, A molecular electronic structure program, Release 2.0, http://www.kjemi.uio.no/software/dalton/dalton.html, 2005.
[39] T. H. Dunning, J. Chem. Phys. **90**, 1007 (1989).
[40] M. Piris, X. Lopez, and J. M. Ugalde, J. Chem. Phys. **126**, 214103 (2007).